A mutation in the *Icsbp1* gene causes susceptibility to infection and a chronic myeloid leukemia–like syndrome in BXH-2 mice

Karine Turcotte,[1,2] Susan Gauthier,[1,2] Ashleigh Tuite,[1,2] Alaka Mullick,[3] Danielle Malo,[2] and Philippe Gros[1,2]

[1]Department of Biochemistry, McGill Cancer Center, and [2]Center for the Study of Host Resistance, Department of Human Genetics, McGill University, Montreal, Quebec H3G 1Y6, Canada
[3]Biotechnology Research Institute, Montreal, Quebec H4P 2R2, Canada

BXH-2 mice develop a fatal myeloid leukemia by a two-step mutagenic process. First, a BXH-2–specific recessive mutation causes a myeloproliferative syndrome. Second, retroviral insertions alter oncogenes or tumor suppressors, resulting in clonal expansion of leukemic cells. We have identified a recessive locus on chromosome 8 (*Myls)* that is responsible for myeloproliferation in BXH-2. This *Myls* interval has been narrowed down to 2 Mb and found to contain several positional candidates, including the *interferon consensus sequence–binding protein 1* gene (*Icsbp,* also known as *interferon regulatory factor 8* [*IRF8*]). We show that BXH-2 mice carry a mutation (915 C to T) resulting in an arginine-to-cysteine substitution at position 294 within the predicted IRF association domain of the protein. Although expression of *Icsbp1* mRNA transcripts is normal in BXH-2 splenocytes, these cells are unable to produce interleukin 12 and interferon-γ in response to activating stimuli, confirming that R294C behaves as a loss-of-function mutation. Myeloproliferation in BXH-2 mice is concomitant to increased susceptibility to *Mycobacterium bovis* (BCG) despite the presence of resistance alleles at the *Nramp1* locus. These results suggest a two-step model for chronic myeloid leukemia in BXH-2, in which inactivation of *Icsbp1* predisposes to myeloproliferation and immunodeficiency. This event is required for retroviral replication, and subsequent insertional mutagenesis that causes leukemia in BXH-2 mice.

CORRESPONDENCE
Philippe Gros:
philippe.gros@mcgill.ca

Abbreviations used: CML, chronic myeloid leukemia; DBD, DNA-binding domain; IAD, IRF association domain; MuLV, murine leukemia virus, SNP, single nucleotide polymorphism.

Chronic myeloid leukemia (CML) is part of a group of six myeloproliferative disorders in humans—that includes polycythemia vera, chronic idiopathic myelofibrosis, essential thrombocythemia, chronic neutrophilic leukemia, and chronic eosinophilic leukemia—which are chronic diseases that can progress to acute leukemia (1–3). CML is generally characterized by the cytogenetically detectable 9:22 translocation known as the Philadelphia (Ph) chromosome, which generates a fusion between the Abelson tyrosine kinase (p145 *ABL*) and the *BCR* gene (breakpoint cluster region; p160 *BCR*; reference 4). However, 5–8% of CML are Ph negative. CML is characterized by an increased number of mature and immature granulocytes in the circulating blood, and, in BM, an increased myeloid/erythroid ratio and a pronounced splenomegaly (1–3). The molecular mechanisms underlying proliferation in Ph-negative CML or in other myeloproliferative disorders remain poorly understood (2). CML can remain indolent for years, but inexorably progresses to an "acceleration" stage (>5% circulating blasts) and a "blastic" stage (>30% blasts), which is rapidly fatal (2–6 mo). Although the mechanisms underlying this evolution are poorly understood, they include inactivation of tumor suppressor genes *p16* (5) and *p53* (5) and of the Rb gene product (6) and include overexpression of EVI-1 (7).

BXH-2 is a recombinant inbred mouse strain derived from C3H/HeJ and C57BL/6J (8) that develops a spontaneous myeloid leukemia uniformly fatal by age one (9–12). The tumors are clonal and caused by insertional mutagenesis of a replication competent B-tropic ecotropic murine leukemia virus (MuLV; references 10–14). In general, mice may carry two types of ecotropic MuLV, either the B-tropic type

The Journal of Experimental Medicine

or the N-tropic type, as defined by the presence of *Fv-1*^{b} (N-tropic restricted) or *Fv-1*^{n} (B-tropic restricted)–restrictive alleles at the *Fv-1* locus on chromosome 4 (13). BXH-2 has two endogenous replication-defective N-tropic ecotropic MuLV proviruses that are designated *Emv1* and *Emv2* on chromosomes 5 and 8, respectively (9). Because BXH-2 mice bear the *Fv-1*^{b} allele, they are not permissive for replication of N-tropic ecotropic viruses. However, they are permissive for replication of B-tropic ecotropic MuLVs and are known to exhibit maternal passage of a B-tropic ecotropic virus that is not integrated in the germline of the strain. Recombination events can modify tropism of ecotropic viruses, and a recombination event between *Emv1* and *Emv2* proviruses, and/or xenotropic virus, is thought to generate the replication-competent B-tropic ecotropic MuLV that causes leukemia in BXH-2 (10–12). BXH-2 leukemia are of myeloid origin, with cells not differentiating beyond the myeloblastic stage being negative for azurophilic granules and myeloperoxidase (10). Interestingly, although other BXH strains (BXH-3, -9, and -12) carry both *Emv1* and *Emv2*, only BXH-2 develops adult onset leukemia (9). In addition, the replication-competent B-tropic ecotropic virus of BXH-2 can induce myeloid leukemia and B cell lymphoma when inoculated into newborns from other permissive BXH strains (10, 11). This suggests that additional BXH-2–specific genetic effects underlie leukemia establishment in these mice.

During the course of an investigation of the unique susceptibility to *Mycobacterium bovis* (BCG) infection of BXH-2 (15), we noted that BXH-2 mice show splenomegaly (spleen index $\approx$ 0.9), which is a phenotype not observed in C57BL/6J and C3H/HeJ progenitors (spleen index $\approx$ 0.5–0.8). In F1 and F2 crosses between BXH-2 and -3 and other inbred strains (C57BL/6J, BALB/cJ, and A/J), splenomegaly behaved as recessive and segregated as a monogenic trait that was given the temporary designation *Myls* (16). Histological analyses showed that homozygosity at *Myls* results in abnormalities in the spleen, LNs, and BM, and, most important, results in the infiltration of Mac1$^+$/Gr1$^+$ granulocyte precursors and the presence of pseudo-Gaucher cells. At 8–16 wk old, hematological parameters of *Myls* (−/−) homozygotes were normal. Expansion of the Mac1$^+$/Gr1$^+$ compartment appeared restricted to the spleen, LNs, and BM at that young age. These results suggested that BXH-2 mice suffer from a myeloproliferative syndrome caused by a mutation (*Myls*) that occurred during the breeding of this strain. A whole genome scan conducted in 187 informative [BALB/cJ × BXH-2]F2 mice localized *Myls* to an 18-cM interval in the distal portion of chromosome 8 near marker *D8Mit13* (LOD > 44; map position 125 Mb; reference 16). Although the *Myls* interval contains many genes, it harbors *Emv2*, one of the two endogenous N-tropic ecotropic MuLV integrated in BXH-2. Because BXH-2 develops B-tropic ecotropic MuLV-induced myeloid leukemia at high frequency, a possible relationship between *Emv2* and *Myls* was investigated. However, *Myls* and *Emv2* appear to be distinct loci because (a) *Myls* is inherited as a recessive trait as opposed to a trait caused by a replication-competent virus, which would be inherited in a dominant fashion; and (b) only a fraction of [A/J × BXH-2]F2 mice homozygous for *Myls* and showing splenomegaly demonstrate B-tropic ecotropic MuLV viral titer in their spleen (16). These results have suggested that BXH-2 carry a recessive loss-of-function mutation at *Myls* that causes initial proliferation of *Mac1*$^+$/*Gr1*$^+$ granulocyte precursors. This proliferation is most likely necessary or provides favorable conditions for a second insertional mutagenesis event that is caused by a replication-competent B-tropic ecotropic MuLV virus, thus resulting in clonal myeloid leukemia typical of BXH-2. The aim of the present study was to use positional cloning to identify the gene and protein underlying the *Myls* effect.

RESULTS

CML-like syndrome in BXH-2 mice

The recombinant inbred mouse strain BXH-2 develops splenomegaly as early as 6 wk old, which is not only characterized by an abundant infiltration of the spleen, but also infiltration of the LNs and the BM, with *Mac1*$^+$/*Gr1*$^+$ myeloid precursors of the granulocytic lineage showing typical ring-shaped nuclei (Fig. 1 A). This phenotype is controlled by a single, BXH-2–specific locus, *Myls*, which is inherited in a recessive manner (Fig. 1 C) and maps on chromosome 8 (16). BXH-2 mice and [A/J × BXH-2]F2 mice homozygotes for *Myls* (−/−) go on to die within 10 mo of age (Fig. 1 B), most probably due to fatal leukemia, compared with control A/J and [A/J × BXH-2]F2 heterozygotes (−/+) or homozygotes (+/+) for wild-type alleles at *Myls* locus (defined by *D8Mit200* and *D8Mit14*) that show 90% survival after 12 mo. This fatal leukemia in *Myls* homozygotes probably involves insertional mutagenesis by a replication-competent B-tropic ecotropic MuLV (10–14). Results in Fig. 1 C show that the splenomegaly phenotype occurs in [C3H × BXH-2]F2 of either *Fv-1*$^{b/b}$ (3/16), *Fv-1*$^{b/n}$ (10/16), or *Fv-1*$^{n/n}$ (3/16) genotypes, the latter of which are not permissive for B-tropic ecotropic MuLV replication (17). Considering that the B-tropic ecotropic MuLV cannot replicate in mice bearing the *Fv-1*^{n} allele, we assume that the splenomegaly phenotype is independent of B-tropic ecotropic MuLV infection and replication.

High resolution linkage map of *Myls*

The minimal genetic interval for *Myls* was initially defined as 9 Mb in size (16), as delineated by *D8Mit200* (map position, 116 Mb) on the proximal side and by *D8Mit13* (map position, 125 Mb) on the distal side (Fig. 2 A). This region contains several candidate genes including *Emv2*, an N-tropic ecotropic MuLV, and the protooncogene *c-maf* in which alterations are associated with certain forms of leukemia (18, 19). Thus, we reduced the minimal genetic interval of the *Myls* locus using additional single nucleotide polymorphism (SNP) markers from the region (*rs3681178*, *mCV23936616*,

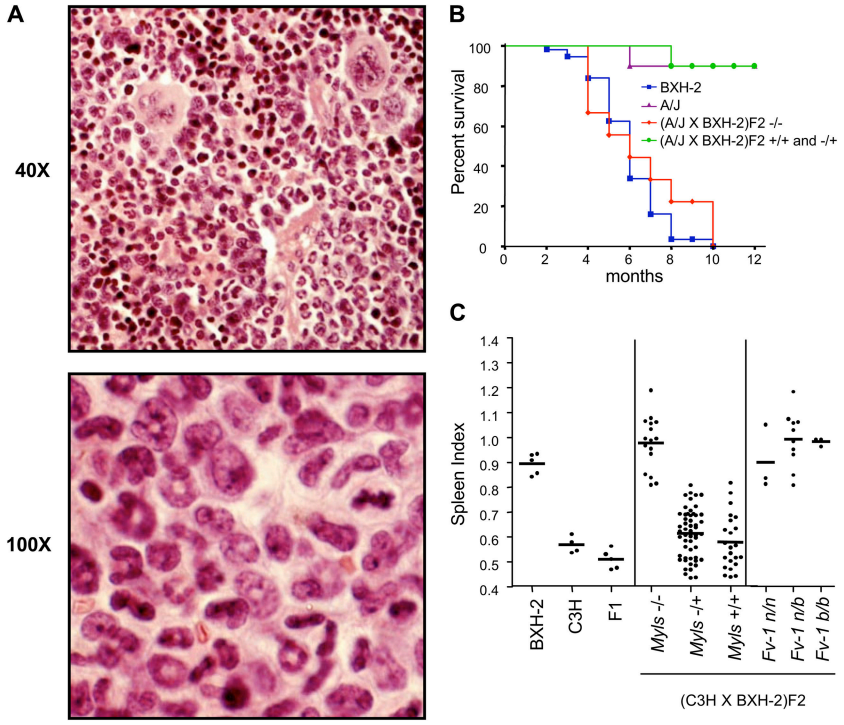

Figure 1. Phenotypic characteristics of the Myls mutation in BXH-2 mice and in F2 mice derived from BXH-2. (A) The *Myls* mutation causes splenomegaly and myeloproliferation. Spleen sections (red pulp) from [BALB/cJ × BXH-2]F2 mice homozygotes for the *Myls* mutation were stained with hematoxylin and eosin and photographed at 40 and 100X magnification. Myeloproliferation in *Myls* mutants involves infiltration of $Mac1^+/Gr1^+$ neutrophil precursors with their characteristic ringlike nuclei. (B) Longevity of A/J, BXH-2, and [A/J × BXH-2]F2 mice according to their *Myls* haplotypes (−/−, homozygote for *Myls*; −/+, heterozygote; and +/+, homozygote wild type, respectively). Myeloproliferation in *Myls* homozygotes results in uniform death of these mice by 10 mo of age. (C) Phenotypic expression of myeloproliferation/splenomegaly in *Myls* homozygotes occurs before, and is independent of, B-tropic ecotropic MuLV virus replication. BXH-2 (−/−), C3H/HeJ (+/+), and [BXH-2 × C3H]F1 controls (+/−), as well as segregating [C3H × BXH-2]F2 mice (8–16 wk old) were phenotyped for splenomegaly, demonstrating the effect of homozygosity at *Myls*. Further classification of *Myls (−/−)* homozygotes according to their genotype for the *Fv-1* locus that controls replication of ecotropic MuLVs shows that splenomegaly occurs in F2 mice permissive ($Fv1^{b/b}$) or not ($Fv1^{b/n}$, $Fv1^{n/n}$) to B-tropic ecotropic MuLV replication.

mCV22708293, and *mCV25191372*) informative between A/J and BXH-2. The allelic combination at these markers was established by nucleotide sequencing in a subgroup of 37 [A/J × BXH-2]F2 mice that shows recombinations between *D8Mit200* and *D8Mit14* and that had been phenotyped for splenomegaly. Our study of these recombinants further reduced the *Myls* interval to ~2 Mb, as delineated by *mCV23936616* on the proximal side (seven crossovers) and by *rs3681178* on the distal side (eight crossovers; Figs. 2 B and 4 D). This analysis excluded *c-maf* and *Emv2* as candidates for *Myls*. Searches of public databases identified a minimum of 14 annotated transcripts in this interval including proteins involved in interaction with different forms of actin (*Cotl1*), cysteine protease (*Uchrp*), cytochrome *c* oxidase (*Cox4a*), interferon-mediated immunity (*Icsbp1/IRF-8*), developmental processes (*Foxf1a*), formation of mesenchymal tissues (*Foxc2*), regulation of Wnt receptor signaling pathway and proteoglycan biosynthesis (*Foxl1*), nonmotor microtubule binding (*Map1lc3*), glycerophospholipid metabolism (*Jph3*), amino acid transport (*Slc7a5*), carbonate dehydratase and lyase (*Car5a*), as well as unknown functions (*Zdhhc7, Noc4, Bdg29*; Fig. 2 C).

Myls is caused by a mutation in *Icsbp/IRF-8* specific to BXH-2

Analysis of candidate genes from the *Myls* interval with respect to the available functional data, and tissue- and cell-specific expression, identified *Icsbp/IRF-8* (*interferon consensus sequence–binding protein/interferon regulatory factor 8*) as a very strong positional candidate. *Icsbp/IRF-8* is a transcription factor member of the IRF family that is expressed in lymphoid organs and is known to play a role in myeloid cell lineage selection (20). *IRF-8* also plays a critical role in mediating transcriptional activation of a group of IFN-γ–responsive genes by binding to specific sequence motifs and recruitment of other transcription factors (21). In splenocytes, *IRF-8* is itself induced by exposure to IFN-γ and LPS (20). The expression of *IRF-8* transcripts was analyzed by Northern blotting in spleens from BXH-2, A/J, and from [A/J × BXH-2]F2 mice showing (Fig. 3 A; high SI, *Myls* −/−) or not splenomegaly (Fig. 3 A; low SI, *Myls* +/+). As previously reported (22),

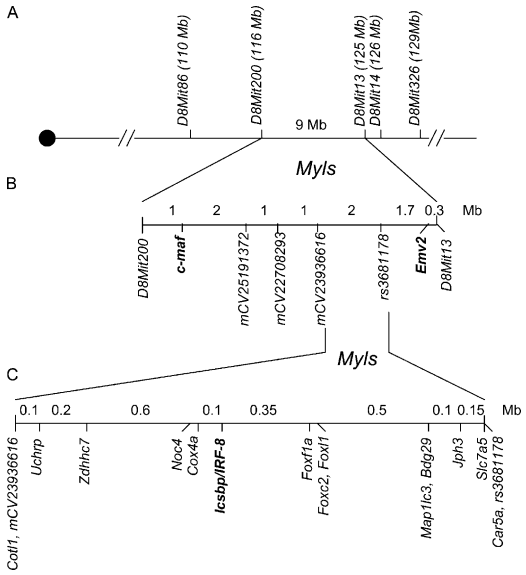

Figure 2. High resolution linkage and physical map of the *Myls* region. (A) Genetic interval for *Myls* was delimited by proximal marker *D8Mit200* and distal marker *D8Mit13*, corresponding to a 9-Mb interval on chromosome 8. The centromere is identified by a large dot. Marker positions (measured in megabases) are based on the Celera Discovery System Online Platform. (B) Fine mapping of *Myls* interval using SNP markers in 37 informative [A/J × BXH-2]F2 mice excluded candidate genes *c-maf* and *Emv2* and reduced the *Myls* candidate interval to 2 Mb with border markers *mCV23936616* and *rs3681178*. Intermarker distances (measured in megabases), based on CDS Online Platform, are shown within each interval (C) The reduced *Myls* interval contains a minimum of 14 known genes present in the NCBI databases and includes the candidate gene *Icsbp/IRF-8*.

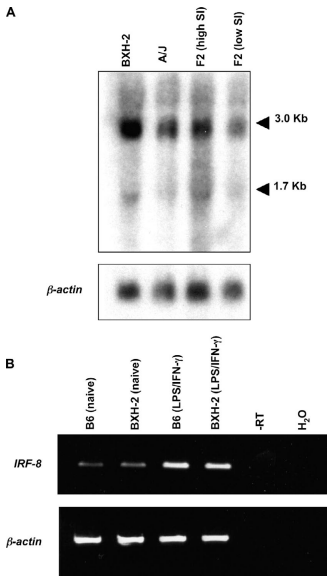

Figure 3. Expression of *IRF-8* RNA in the spleens of A/J, B6, BXH-2, and BXH-2–derived F2 mice. (A) Total RNA was extracted from the spleens of BXH-2 (−/−), A/J (+/+), and [A/J × BXH-2]F2 animals displaying (high SI; −/−) or not displaying (low SI; +/+) splenomegaly, was analyzed by Northern blotting with a cDNA fragment corresponding to part of the DBD (from +179 to +326) of *IRF-8*, and used as a hybridization probe. (B) RT-PCR analysis of *IRF-8* mRNA expression in splenocytes from C57BL/6J and BXH-2 either before (naive) or after treatment with LPS and IFN-γ. β-Actin mRNA expression was used as an internal control. Products from RT-PCR reactions performed in the absence of reverse transcriptase (−RT) or in the absence of RNA template (H_2O) were included as negative controls, and all PCR products were analyzed by agarose gel electrophoresis.

the *IRF-8* gene produces two transcripts in the spleen of ~3.0 and 1.7 Kb, respectively. Neither the size nor the relative abundance of the *IRF-8* transcripts in spleen appeared to be affected by the *Myls* mutation when compared with the β-actin that was used as control (Fig. 3 A). Similar results were obtained by semi-quantitative and quantitative analysis using RT-PCR (Fig. 3 B and not depicted). Likewise, *IRF-8* mRNA transcripts could be induced in splenocytes after LPS/IFN-γ stimulation (Fig. 3 B), and this induction was similar in normal (C57BL/6J) and in *Myls* mutant mice (BXH-2).

Members of the IRF family share a highly conserved, COOH-terminal, DNA-binding domain (DBD) that contains a characteristic conserved tryptophan repeat and binds to similar DNA sequences, termed IRF element, interferon-stimulated response element, interferon consensus sequence, or Ets-IRF composite elements present in the promoter of target genes (23). The COOH-terminal portion of the protein contains a trans-activation domain, the IRF association domain (IAD), which is poorly conserved and is implicated in recruiting other transcription factors including members of the IRF family to assemble a transcriptional complex (23). Nucleotide sequencing of the *IRF-8* transcript (Fig. 4 A) from BXH-2 identified a C-to-T substitution at position 915 of the cDNA, causing an arginine-to-cysteine replacement at amino acid position 294 (R294C) within the predicted IAD domain of the protein (Fig. 4 B). This polymorphism appears specific for BXH-2 and is absent in the C57BL/6J parent, from which the *Myls-IRF-8* portion of chromosome 8 in BXH-2 is derived (Fig. 4 A). The R294C substitution in *IRF-8* modifies a HaeIII restriction site in genomic DNA that provides a convenient genomic marker for the mutation (Fig. 4 C). A total of 12 standard inbred mouse strains (including C57BL/6J and C3H/HeJ parents; unpublished data), together with the 11 available BXH strains were genotyped for the HaeIII polymorphism (Fig. 4 C). None of the strains tested displayed the R294C-specific variant, verifying that $IRF\text{-}8^{C294}$ is unique to BXH-2. Additional segregation analysis in the 37 [A/J × BXH-2]F2 mice exhibiting recombination between *D8Mit200* and *D8Mit14* in the *Myls* interval showed complete concordance between *IRF-8* alleles (determined by the HaeIII polymorphism) and the presence or absence of splenomegaly (Fig. 4 D, hatched boxes [high SI] and empty boxes [low SI]). Finally, R294 is conserved in the chicken and human IRF-8 protein homologues, and R294C is a non-conservative substitution removing a positive charge at the

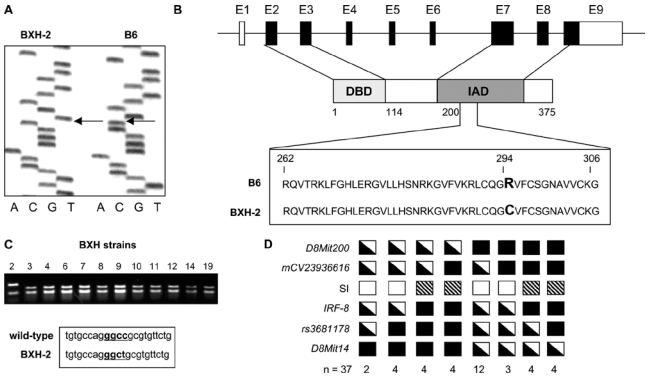

Figure 4. The *IRF-8* gene is mutated in BXH-2 mice. (A) Coding exons of *IRF-8* gene were completely sequenced in C57BL/6J and BXH-2 mice. A C-to-T mutation at cDNA position 915 within exon 7 was found in BXH-2 mice. (B) Genomic organization of the *IRF-8* gene, including the position of individual noncoding (open boxes) and coding (closed boxes) exons (E1–E9). The position of individual coding exons with respect to known structural features of the IRF-8 protein, including the DNA-binding domain (DBD) and the IRF association domain (IAD), is shown. The C915T nucleotide substitution results in an Arg-to-Cys change at amino acid position 294 of the protein (R294C) in the IAD, which is shown as an alignment of the B6 and BXH-2 sequences in this region. (C) C915T disrupts a HaeIII restriction site (ggcc) in genomic DNA that can be assayed by PCR amplification, digested by HaeIII, and analyzed by agarose gel electrophoresis. Analysis of the BXH strains set (numbered 2–19) indicates that C915T mutation is specific for BXH-2. (D) Haplotype map of the 37 [A/J × BXH-2]F2 mice showing single recombination events between *D8Mit200* and *D8Mit14* that were used to define the *Myls* interval. Each column represents a chromosomal haplotype and the total number of animals bearing this haplotype is indicated at the bottom (*n*). For genetic markers *D8Mit200*, *mCV23936616*, *IRF-8*, *rs3681178*, and *D8Mit14*, homozygosity for BXH-2 (closed boxes, C57BL/6J derived) or heterozygosity (half-shaded boxes) is identified. The presence (hatched boxes, high SI) or absence (open boxes, low SI) of splenomegaly is shown.

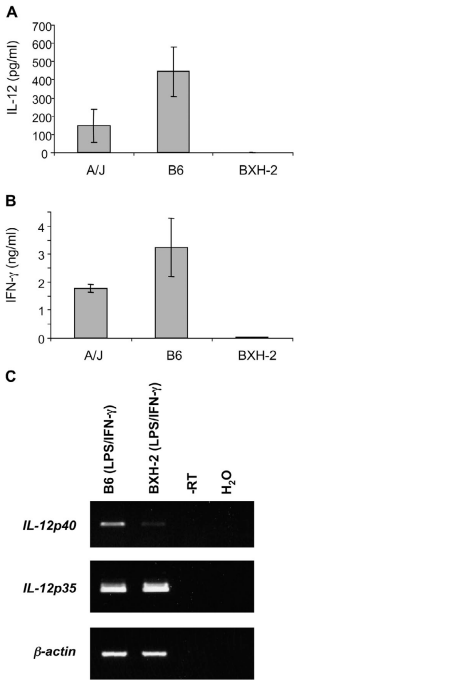

Figure 5. Effect of *IRF-8*^{C294} mutation on IL-12 and IFN-γ production. Spleen cells from A/J, C57BL/6J (B6), and BXH-2 mice were harvested and cultured in the presence of either LPS only (100 ng/ml; B), or LPS (100 ng/ml) and IFN-γ (200 U/ml; A and C) for 24 h, and the levels of IL-12 and IFN-γ were determined in the culture supernatant by ELISA. In parallel, RNA was extracted from cultured splenocytes and used as a template to monitor the levels of expression of *IL-12p40*, *IL-12p35*, and β-*actin* transcripts by RT-PCR. RT-PCR reaction products were analyzed by gel electrophoresis as described in the legend for Fig. 3. The error bars in A and B represent the SEM.

294 position and introducing a smaller residue with a potential for disulfide bonding. Although R294 is not conserved in other members of the mouse IRF protein family, a basic residue is usually found at this position with the exception of ISGF3γ that harbors a proline (24). An induced mutation at position 289 (R289E) in IRF-8, within an α helix of the IAD domain, was previously shown to disrupt the interaction of IRF-8 with PU.1 (25), demonstrating the importance of this region for transactivation. Together, these results establish that *IRF-8*^{C294} is a new mutation that appeared on the B6 background of BXH-2 and became fixed during the inbreeding of this strain. This mutation is either tightly linked or identical to *Myls*.

IRF-8^{C294} impairs cytokine production by BXH-2 splenocytes

We next investigated the effect of the R294C substitution on IRF-8 protein activity. IRF-8 is known to be essential for transcriptional activation of the *IL-12p40* subunit gene, and for the production of IL-12 and IFN-γ by splenocytes in response to LPS stimulation (26). Thus, splenocytes from BXH-2 (*IRF-8*^{C294}) and from C57BL/6J and A/J controls (*IRF-8*^{R294}) were harvested and stimulated with either LPS (100 ng/ml) or with LPS (100 ng/ml) + IFN-γ (200 U/ml). Production of IL-12 (LPS + IFN-γ treatment; Fig. 5 A) and IFN-γ (LPS treatment; Fig. 5 B) was monitored in culture supernatants by ELISA, and RNA was extracted from the stimulated cells for analysis of *IL-12p40* and *IL-12p35* mRNA production by RT-PCR (Fig. 5 C). Although stimulation caused IL-12 and IFN-γ production by control A/J and B6 splenocytes, BXH-2 spleen cells did not secrete detectable amounts of IL-12 and IFN-γ in response to the same treatments. Failure of BXH-2 splenocytes to secrete IL-12 was associated with reduced transcriptional activation of the *IL-12p40* gene when compared with B6, and as estimated by semi-quantitative RT-PCR (Fig. 5 C) and quantitative RT-PCR (not depicted). Together, these results demonstrate that the IRF-8^{C294} protein isoform is functionally impaired in BXH-2, and can no longer mediate transcriptional activation of IFN-γ responsive genes.

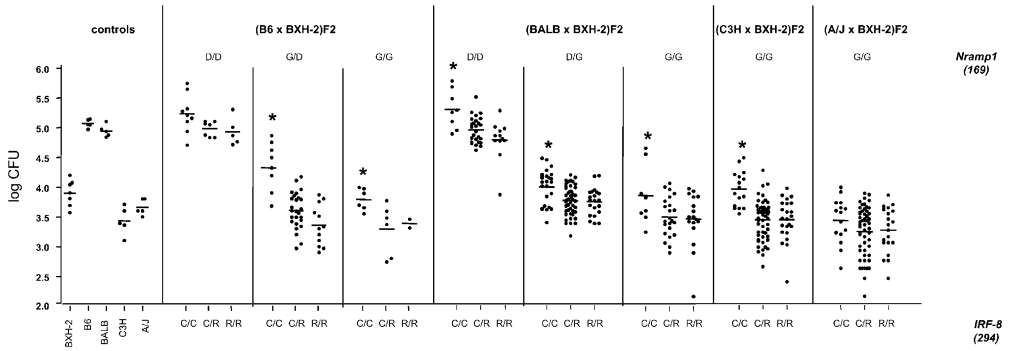

Figure 6. Effect of *IRF-8*^{C294} mutation on Nramp1-dependent replication of *M. bovis* (BCG) in the spleen of segregating BXH-2–derived F2 mice. Parental strains BXH-2 (*IRF-8*^{C294}, *Nramp1*^{G169}) and BCG-susceptible C57BL/6J and BALB/cJ (*IRF-8*^{R294}, *Nramp1*^{D169}), or BCG-resistant C3H/HeJ and A/J control strains (*IRF-8*^{R294}, *Nramp1*^{G169}) were infected with *M. bovis* (BCG), and spleen CFU counts were determined 3 wk later. F1 and F2 crosses were derived from BXH-2 and either C57BL/6J (B6), BALB/cJ (BALB), C3H/HeJ (C3H), or A/J, in the combinations indicated at the top of each graph. F2 mice were genotyped for *Nramp1* (G, resistant; D, susceptible) and for *IRF-8* alleles (C, mutant; R, wild type) and separated according to their haplotype combinations. The allelic status for *Nramp1* and for *IRF-8* is indicated at the top and bottom of the graphs, respectively. Dots represent individual mice, and means for each group are shown as lines on the graph. Asterisks indicate that the effect of homozygosity for *IRF-8*^{C294} is statistically significant in that *Nramp1* haplotype group ($P < 0.05$, unpaired Student's *t* test).

IRF-8^{C294} increases susceptibility to intracellular infection in BXH-2

Nramp1 functions as a pH-dependent metal (e.g., Fe^{2+}, Mn^{2+}, and Zn^{2+}) efflux system at the phagosomal membrane of macrophages to prevent intracellular replication of different pathogens (27). *Nramp1* mutations abrogate resistance to infection with *Mycobacterium*, *Salmonella*, and *Leishmania* species in mice (28). Inbred mouse strains harbor either a susceptibility (*Nramp1*^{D169}; C57BL/6J, BALB/cJ) or a resistance (*Nramp1*^{G169}; C3H/HeJ, A/J, DBA/2) allele at *Nramp1*, with susceptibility being fully recessive (29). Although BXH-2 mice bear a C3H-derived resistance *Nramp1* allele (G169), they show increased susceptibility to infection with *M. bovis* (BCG) (reference 15). The susceptibility phenotype of BXH-2 is variable, with spleen CFU counts at the peak of infection being between 5- (Fig. 6) and 100-fold (15) superior to those seen in parental C3H controls. This variability appears to be related, in part, to the age at which BXH-2 mice are tested, and possibly linked to the appearance of leukemia. To monitor the possible effects of loss of function at *IRF-8* on resistance to *M. bovis* (BCG) infection, a number of F2 crosses were derived between BXH-2 (*IRF-8*^{C294}, *Nramp1*^{G169}) and other inbred strains fixed for either susceptibility (D169; C57BL/6J, BALB/cJ) or resistance (G169; A/J, C3H/HeJ) alleles at *Nramp1*. Spleen CFU counts 3 wk after i.v. infection with 2×10^4 live *M. bovis* (BCG) were determined, and the effect of wild-type (R294) or mutant (C294) alleles at *IRF-8* on *Nramp1*-determined resistance (G/G and G/D) or susceptibility (D/D) to infection was evaluated (Fig. 6). Homozygosity for the mutant *IRF-8*^{C294} allele was found to be associated with increased mycobacterial replication in most F2 animals (Fig. 6), irrespective of their parental origins or *Nramp1* genotype. The effect was most obvious in resistant animals either homozygous (G/G) or heterozygous (G/D) for *Nramp1* resistance alleles, and caused a five- to eightfold increase in spleen CFUs, depending on the cross that was analyzed. The mutant *IRF-8*^{C294} allele effect on bacterial replication was completely recessive, which was in agreement with the loss of activity seen for C294 in functional assays (Fig. 5). These results indicate that loss of IRF-8 function in BXH-2 not only predisposes mice to leukemia, but also increases susceptibility to infection with an intracellular pathogen.

DISCUSSION

We have used a positional cloning approach to identify the mutation that underlies the myeloproliferative disorder characteristic of BXH-2. High resolution linkage mapping in a large number of informative mice succeeded in excluding two positional candidates, *Emv2* and *c-maf*. *Emv2* corresponds to an integrated copy of a replication-defective N-tropic ecotropic MuLV virus (30, 31), and the acute leukemia of BXH-2 is known to be caused by a replication-competent B-tropic recombinant ecotropic MuLV virus (9, 10, 12). The protooncogene *c-maf* is deregulated in certain tumors, including multiple myeloma (32). Instead, our studies suggest that *IRF-8* is the gene affected in BXH-2 because of the following: (a) *IRF-8* maps within the minimal 2-Mb genetic interval of *Myls*; (b) *IRF-8* is known to play a critical role in monocyte maturation, and *IRF-8*-deficient mice show a proliferation of granulocytes (26) and are immunocompromised (33, 34); (c) myeloproliferation in BXH-2 is associated with a sequence variant (R294C) in IRF-8 that is unique to BXH-2, and is neither found in other BXH strains nor found in other inbred strains, which affects a charge that is conserved in other members of the IRF family; and (d) as opposed to controls, spleen cells expressing the IRF-8^{C294} variant cannot produce IFN-γ and IL-12 in response to LPS.

These findings elucidate the molecular basis of the unique CML-like disease of BXH-2 mice, and they establish BXH-2 as a valuable mouse model to study the two-step process underlying onset and progression of CML and other myeloproliferative disorders. In humans, CML is typified by an initial chronic period with predominant granulocytic involvement, and this is followed by an advancement and rapidly fatal blast crisis that is characterized by clonal expansion of leukemic cells. In BXH-2, the initial chronic phase is caused by the R294C loss-of-function mutation in IRF-8 that occurred during the breeding of this strain. These results suggest a tumor suppressor status of IRF-8 in myeloid leukemia (35), and agree with recent results showing that IRF-8 can antagonize the pro-neoplastic effect of ABL-BCR fusions (36–38). Although loss of function at IRF-8 is necessary for leukemia in BXH-2, it does not appear to be sufficient.

A second mutagenic event is provided by insertional mutagenesis with a replication-competent B-tropic ecotropic MuLV virus, which results in inactivation of additional tumor suppressors and/or activation of protooncogenes, leading to rapid expansion of clonal tumors in these mice (14, 39). This two-step model explains why (a) other BXH strains that carry *Emv1* and *Emv2* copies but are wild type for *IRF-8* do not develop leukemia, and (b) that the replication-competent B-tropic ecotropic virus of BXH-2 can induce myeloid leukemias and B cell lymphomas when inoculated into newborns of other mouse strains (10, 11). Thus, the myeloproliferative syndrome associated with inactivation of *IRF-8* appears to be necessary for the production of a replication-competent B-tropic ecotropic virus. Indeed, we have previously reported that although ~50% of [A/J × BXH-2]F2 mice homozygote at *Myls* (−/−) have detectable virus in their spleen, none of [A/J × BXH-2]F2 mice either heterozygote (*Myls*/+) or homozygote (+/+) wild type show B-tropic ecotropic MuLV in their spleen when tested by XC plaque assay (16). This facilitation could be achieved through enhanced replication of *Emv1/Emv2*, such as that recently documented for the hepatitis C virus replicons in Huh7 cells where IRF-1 expression was reduced (40), or through an increased probability of recombination event between RNA transcripts produced by the replication-defective *Emv1* (mutated in *env*) and *Emv2* (mutated in *pol*) proviruses provided by the cellular background of actively replicating $Mac1^+$/$Gr1^+$ cells, or both. Although other genetic and environmental factors may also favor progression of $IRF\text{-}8^{C294}$ cells to malignant transformation, the virally dependent insertional mutagenesis event of BXH-2 appears to be both more efficient and more rapid path to acute leukemia. Indeed, [129 × C57BL/6J] mice lacking endogenous replication-competent retrovirus but carrying a null mutation at *IRF-8*, show a very similar pathology (hepato-splenomegaly, myeloproliferation of $Mac1^+/GR1^+$ cells, presence of pseudo-Gaucher cells), but significantly reduced mortality (33% mortality by 50 wk; reference 26) when compared with BXH-2 (100% mortality by 40 wk). In addition, these aging [129 × C57BL/6J] mice also develop histiocytic sarcomas (41), which are indicative of strain background effects on disease. Together, these results highlight the possible importance of *IRF-8* in the etiology of human leukemia.

BXH-2 mice show increased susceptibility to infection with *M. bovis* (BCG) (15), despite the presence of a resistance allele at *Nramp1*(G169). This phenotype is variable (15 and unpublished data), age dependent, and may be secondary to the onset of acute leukemia in these mice, as opposed to a direct effect of *IRF-8* mutation. The effect of *IRF-8* mutation on the susceptibility to *M. bovis* (BCG) was studied in animals derived from four different F2 crosses between BXH-2 and other inbred mouse strains of resistant or susceptible *Nramp1* genetic background. As opposed to infection with intracellular pathogens *Toxoplasma gondii* (33) and *Leishmania major* (34), where loss of function at *IRF-8* causes acute susceptibility, the $IRF\text{-}8^{C294}$ allele did not abrogate the major protective effect of *Nramp1* at peak of infection (3 wk after infection). Instead, homozygosity for $IRF\text{-}8^{C294}$ caused a moderate increase in CFU counts in the spleen at the peak of infection, and this was true for all three *Nramp1* genotypes studied. Thus, *IRF-8* appears to act as a true modulator of *Nramp1* expression or function. The effect could be indirect, through reduced production of IL-12 and IFN-γ, two cytokines that play a critical role in host defenses against mycobacterial infections, or could be direct through transcriptional regulation of the *Nramp1* gene, the promoter of which contains interferon response elements. Although additional experiments will be required to distinguish the two possibilities, these results raise the possibility that naturally occurring polymorphic variants in human *IRF-8* may act as predisposing factors for susceptibility to mycobacterial infections (leprosy and tuberculosis) in areas of endemic disease.

IRF-8 is a member of the IRF family whose common structural features include a DBD and an IAD (23). The DBD only binds DNA by interacting with other transcription factors, including other members of the IRF family (21). Deletion studies have shown that the IAD mediates interaction with other proteins. Both an α helix with amphipathic character at position Ser^{325}-Phe^{334} and phosphorylation of a serine at position 260 (Ser^{260}) are known to be essential for interaction of IRF-8 with other IRFs (21). The R294C mutation of BXH-2 maps in the IAD region and affects a residue whose positive charge has been conserved in other IRF proteins. In addition, R294C maps within a well-conserved portion of the otherwise divergent IAD, which is immediately downstream the Arg-Leu-Cys motif that is precisely conserved in IRF-4, -5, -6, -8, and -9 (21). The R-to-C replacement is not conservative and results in the loss of a positive charge, which may play an important structural or functional role. In addition, it introduces a sulfhydryl side chain at that position with the potential to form a highly disruptive disulfide bond with other neighboring cysteine residues. Thus, this mutation may affect interaction with other IRF proteins and may prevent formation of a transcription-

ally active DNA binding complex. Although speculative, this proposal is in agreement with the noted inability of IRF-8^{C294} to mediate induction of target genes such as *IL-12p40* in response to LPS and IFN-γ stimulation. Finally, IRF-8^{C294} maps near R289E, a mutation within the α helix of the IAD domain that was recently shown to disrupt the interaction of IRF-8 with PU.1 (25), demonstrating the importance of this region for transactivation. Additional experiments are currently being conducted to determine the molecular basis for the loss of function in IRF-8^{C294}.

MATERIALS AND METHODS

Animals. Inbred C57BL/6J, BALB/cJ, C3H/HeJ, and A/J mice were purchased from the Jackson Laboratory. Recombinant inbred BXH-2 male mice were originally obtained from the Jackson Laboratory (as single male animals in the mid-1990's) and were used to generate F2 crosses with BALB/cJ, C57BL/6J, and A/J mice that were phenotyped for the presence of splenomegaly and their susceptibility to *M. bovis* (BCG) infection. An independent BXH-2 stock (a gift from N. Copeland and N. Jenkin, National Cancer Institute, Frederick, MD) was obtained in the early 2000's and was subsequently maintained as a breeding colony at McGill University. This latter stock was used to produce additional F2 crosses that were used for high resolution linkage mapping of *Myls*. F2 progeny were produced by systematic brother–sister mating, with no gender bias. Maintenance and experimental manipulation of animals were performed according to the guidelines and regulations of the Canadian Council on Animal Care.

Histology. Spleens were harvested from [A/J × BXH-2]F2 mice at least 3 mo old. Tissues were fixed in Bouin's solution (9 g/liter picric acid, 4% acetic acid, 4% formaldehyde, and 4% methanol), embedded in paraffin, and sectioned as we have described previously (16). 5-μm sections were stained with hematoxylin and eosin and photographed at 40 and 100× magnification.

Genotyping. Genomic DNA was prepared from tail biopsies by incubating in lysis buffer (100 mM Tris-HCl, pH 8.0, 5 mM EDTA, pH 8.0, 200 mM NaCl, and 0.2% SDS) containing 0.5 mg/ml proteinase K (at 55°C for 16 h) followed by phenol/chloroform extraction and precipitation with isopropanol (42). Primer pairs defining dinucleotide repeat markers—*D8Mit200*, *D8Mit14*, and *D8Mit13* (*Myls* locus)—were obtained from Invitrogen, or in the case of *D1Mcg2* and *D1Mcg4* (*Nramp1*), were synthesized in-house. Marker positions in this study were those from the Mouse Genome Assembly, presented at the University of California Santa Cruz Bioinformatics website or the Celera Discovery System Online Platform. Sequence length polymorphisms were genotyped by a standard PCR-based method using α-[^{32}P]dATP labeling and separation on denaturing 9% polyacrylamide gels (42). SNPs from the *Myls* region and informative for A/J and C57BL/6J (BXH-2) were obtained from the Celera Discovery System and Celera's associated databases (*mCV25191372*, *mCV22708293*, and *mCV23936616*) and from the National Center for Biotechnology Information (NCBI) dbSNP database (*rs3681178*). Primer pairs defining each SNP were designed and used for PCR amplification using genomic DNA as a template. The PCR products were subjected to cycle sequencing using fluorescently labeled BigDye Terminator and an automated ABI3700 instrument (Applied Biosystems).

Sequencing of *IRF-8* and alleles identification. The transcript map of the chromosome 8 region overlapping *Myls* was obtained from the Mouse Genome Assembly using the University of California Santa Cruz Bioinformatics web browser. Individual coding exons of *IRF-8* were obtained by standard PCR amplification using primer pairs derived from intronic sequences, and genomic DNA from C57BL/6J and BXH-2 as templates. PCR products were subjected to cycle sequencing using fluorescently labeled BigDye Terminator, and an automated ABI3700 instrument. Sequences were validated by standard dideoxynucleotide sequencing using α-[^{33}P]dATPs (43). A single nucleotide polymorphism (C915T; Arg294Cys) was identified in exon 7 of the *IRF-8* gene of BXH-2. This sequence variant abolishes a HaeIII cleavage site (5′-ggcc-3′) in BXH-2, which can be scored by HaeIII digestion of a 397-bp exon 7 fragment generated by PCR amplification of genomic DNA with the oligonucleotide primer pair 5′-gct ccc cat ctt cta ggc-3′ and 5′-acc acc tcg tcc cgc tc-3′, followed by separation on 2% agarose gel and visualization of ethidium bromide–stained products under UV.

Cytokine production. Mice were killed under anesthesia and spleens were removed aseptically. Spleen cell suspensions were obtained by gently disrupting the tissue by passing though a 70-μm mesh in 3 ml RPMI 1640 medium supplemented with 10% heat-inactivated FBS, 2 mM glutamine, 100 U/ml penicillin, 50 μg/ml streptomycin (GIBCO BRL), 10 mM Hepes, pH. 7.6, and 5 mM β2-mercaptoethanol. Splenocytes were obtained after incubation of spleen cells with hemolytic Gey's solution as described previously (44). They were seeded in tissue culture vessels at 5×10^6 cells/ml followed by incubating with phenol-extracted LPS from *Escherichia coli* O55:B5 (100 ng/ml; Sigma-Aldrich) and murine recombinant IFN-γ (200 U/ml; Sigma-Aldrich) for 24 h at 37°C. Tissue culture supernatants from LPS/IFN-γ or LPS-stimulated cells were collected and assayed for IL-12 and IFN-γ production, respectively, using a commercially available (BD Biosciences), "two-site sandwich" ELISA kit. Total cellular RNA was isolated using a commercial TRIzol reagent (Life Technologies).

Northern blot. Mice were killed under anesthesia, and the spleens were removed and rapidly frozen in liquid nitrogen. Frozen spleens were placed in TRIzol reagent and were immediately homogenized by mechanical disruption with a polytron homogenizer (Kinematica), and RNA was further extracted according to the protocol provided by the manufacturer. Total spleen RNA (10 μg per lane) was analyzed by electrophoresis on a denaturing agarose (1.2%) gel containing 4% formaldehyde, this was followed by blotting onto a hybridization membrane. The blot was prehybridized and hybridized (for 16 h each at 65°C) in the same buffer consisting of 1% SDS, 1 M NaCl, and 10% dextran sulfate. Hybridization was performed with an *IRF-8* cDNA fragment (nucleotide positions 179–326) labeled to high specific activity by random priming with 3,000 Ci/mmol α-[^{32}P]dATP (Perkin-Elmer). Blots were washed to a final stringency of 0.5× SSC (20× SSC is 3 M sodium chloride and 0.3 M sodium citrate, pH 7.0), 0.5% SDS, for 30 min at 65°C, and exposed to film (BioMax MS; Kodak).

mRNA expression studies by RT-PCR. The level of mRNA expression of different genes was measured by PCR amplification of cDNA transcripts generated by reverse transcriptase (RT-PCR), as we have described previously (45). For cDNA synthesis, total spleen RNA (2 μg) was reverse transcribed using 200 U/reaction Moloney MuLV reverse transcriptase (Invitrogen) in a 20-μl reaction mixture containing 50 mM Tris, pH 8.3, 3 mM $MgCl_2$, 75 mM KCl, 5 ng/μl of randomhexamers, deoxyribonucleotides triphosphates (dNTPs; 0.5 mM each), 10 mM DTT, and 36 U of placental RNase inhibitor (RNAguard; Amersham Biosciences) for 50 min at 37°C. Upon completion of reverse transcriptase reaction, the cDNA mixture was diluted 1:10, of which 2 μl was used as a template for PCR amplification using gene-specific oligonucleotide primer pairs corresponding to *IL-12p40* (5′-gtg aag cac caa att act ccg g-3′; 5′-gct tca tca tct gca agt tct tgg g-3′), *IL-12p35* (5′-ggc tac tag aga gac ttc ttc c-3′; 5′-gtg aag cag gat gca gag ctt c-3′), *IRF-8* (5′-caa tca gga ggt gga tgc ttc-3′; 5′-gtc agt cac ttc ttc aaa atc tg-3′), and β-*actin* (5′-aac tgg gac gac atg gag aag-3′; 5′-acc aga ggc ata cag gga caa-3′). Reaction conditions for PCR were those recommended by the manufacturer of Taq DNA polymerase (Invitrogen), adjusted to 1.4 mM $MgCl_2$, 0.1 mM dNTPs, 1 U Taq DNA polymerase, and 0.3 μM oligonucleotide primers in a final volume of 25 μl. Parameters for PCR amplification were 30 s at 94°C, 30 s at 58°–61°C (depending on primmer pair), 30 s at 72°C for 28–30 cycles, followed by a final step at 72°C for 7 min. The cDNAs were analyzed by electrophoresis on a 1.4% agarose gel containing ethidium bromide and were photographed under UV light.

Infection with *M. bovis* (BCG). *M. bovis* (BCG, strain Montreal) was passed in vitro and prepared for in vivo infections as described previously (46). 2×10^4 CFU was used to i.v. inoculate mice (2–4 mo old). 21 d after infection, mice were killed, weighed, and the degree of infection was assessed by determination of spleen CFU, as previously described (47). The index of BCG infection was defined as the logarithm of the mean number of viable BCG recovered from spleens. The spleen index (SI) was determined as the square root of spleen weight (×100) divided by the body weight.

We thank Miria Elias, Melissa Mathieu, and Patrick Fortin for technical help.

This project was supported by research grants to P. Gros from Canadian Genetic Diseases Network and the Société de Recherche sur le Cancer Inc. P. Gros is a James McGill Professor of Biochemistry. K. Turcotte was supported by studentships from the Fonds de la Recherche en Santé du Québec, and the Canadian Institutes of Health Research (CIHR). D. Malo is a Scholar of CIHR and an International Research Scholar of the Howard Hughes Medical Institute.

The authors have no conflicting interests.

Submitted: 20 October 2004
Accepted: 5 January 2005

REFERENCES

1. National Cancer Institute. "Chronic myelogenous leukemia." http://www.nci.nih.gov/cancerinfo/pdq/treatment/cml.
2. Cortes, J., and M.E. O'Dwyer. 2004. Clonal evolution in chronic myelogenous leukemia. *Hematol. Oncol. Clin. North Am.* 18:671–684.
3. Beutler, E., M.A. Lichtman, B.S. Coller, T.J. Kipps, and U. Seligsohn. 2001. Williams Hematology. McGraw-Hill Medical Publishing Division, New York. 1941 pp.
4. Deininger, M.W., J.M. Goldman, and J.V. Melo. 2000. The molecular biology of chronic myeloid leukemia. *Blood.* 96:3343–3356.
5. Sill, H., J.M. Goldman, and N.C. Cross. 1995. Homozygous deletions of the p16 tumor-suppressor gene are associated with lymphoid transformation of chronic myeloid leukemia. *Blood.* 85:2013–2016.
6. Towatari, M., K. Adachi, H. Kato, and H. Saito. 1991. Absence of the human retinoblastoma gene product in the megakaryoblastic crisis of chronic myelogenous leukemia. *Blood.* 78:2178–2181.
7. Ogawa, S., K. Mitani, M. Kurokawa, Y. Matsuo, J. Minowada, J. Inazawa, N. Kamada, T. Tsubota, Y. Yazaki, and H. Hirai. 1996. Abnormal expression of Evi-1 gene in human leukemias. *Hum. Cell.* 9:323–332.
8. Taylor, B.A. 1978. Recombinant inbred strains: use in gene mapping. *In* Origins of Inbred Mice. Herbert C. Morse III, editor. Academic Press, New York. 423–438.
9. Jenkins, N.A., N.G. Copeland, B.A. Taylor, H.G. Bedigian, and B.K. Lee. 1982. Ecotropic murine leukemia virus DNA content of normal and lymphomatous tissues of BXH-2 recombinant inbred mice. *J. Virol.* 42:379–388.
10. Bedigian, H.G., D.A. Johnson, N.A. Jenkins, N.G. Copeland, and R. Evans. 1984. Spontaneous and induced leukemias of myeloid origin in recombinant inbred BXH mice. *J. Virol.* 51:586–594.
11. Bedigian, H.G., L.A. Shepel, and P.C. Hoppe. 1993. Transplacental transmission of a leukemogenic murine leukemia virus. *J. Virol.* 67: 6105–6109.
12. Bedigian, H.G., B.A. Taylor, and H. Meier. 1981. Expression of murine leukemia viruses in the highly lymphomatous BXH-2 recombinant inbred mouse strain. *J. Virol.* 39:632–640.
13. Lilly, F., and T. Pincus. 1973. *Genetic control of murine viral leukemogenesis*. Advances in Cancer Research, vol. 17, Georges Klein and Sidney Weinhouse, editors. New York: Academic Press.
14. Li, J., H. Shen, K.L. Himmel, A.J. Dupuy, D.A. Largaespada, T. Nakamura, J.D. Shaughnessy Jr., N.A. Jenkins, and N.G. Copeland. 1999. Leukaemia disease genes: large-scale cloning and pathway predictions. *Nat. Genet.* 23:348–353.
15. Skamene, E., P. Gros, A. Forget, P.A. Kongshavn, C. St. Charles, and B.A. Taylor. 1982. Genetic regulation of resistance to intracellular pathogens. *Nature.* 297:506–509.
16. Turcotte, K., S. Gauthier, L.M. Mitsos, C. Shustik, N.G. Copeland, N.A. Jenkins, J.C. Fournet, P. Jolicoeur, and P. Gros. 2004. Genetic control of myeloproliferation in BXH-2 mice. *Blood.* 103:2343–2350.
17. Jolicoeur, P. 1979. The Fv-1 gene of the mouse and its control of murine leukemia virus replication. *Curr. Top. Microbiol. Immunol.* 86:67–122.
18. Chesi, M., P.L. Bergsagel, O.O. Shonukan, M.L. Martelli, L.A. Brents, T. Chen, E. Schrock, T. Ried, and W.M. Kuehl. 1998. Frequent dysregulation of the c-maf proto-oncogene at 16q23 by translocation to an Ig locus in multiple myeloma. *Blood.* 91:4457–4463.
19. Chesi, M., W.M. Kuehl, and P.L. Bergsagel. 2000. Recurrent immunoglobulin gene translocations identify distinct molecular subtypes of myeloma. *Ann. Oncol.* 11(Suppl):131–135.
20. Tamura, T., and K. Ozato. 2002. ICSBP/IRF-8: its regulatory roles in the development of myeloid cells. *J. Interferon Cytokine Res.* 22:145–152.
21. Levi, B.Z., S. Hashmueli, M. Gleit-Kielmanowicz, A. Azriel, and D. Meraro. 2002. ICSBP/IRF-8 transactivation: a tale of protein-protein interaction. *J. Interferon Cytokine Res.* 22:153–160.
22. Kanno, Y., C.A. Kozak, C. Schindler, P.H. Driggers, D.L. Ennist, S.L. Gleason, J.E. Darnell Jr., and K. Ozato. 1993. The genomic structure of the murine ICSBP gene reveals the presence of the gamma interferon-responsive element, to which an ISGF3 alpha subunit (or similar) molecule binds. *Mol. Cell. Biol.* 13:3951–3963.
23. Nguyen, H., J. Hiscott, and P.M. Pitha. 1997. The growing family of interferon regulatory factors. *Cytokine Growth Factor Rev.* 8:293–312.
24. Ortiz, M.A., J. Light, R.A. Maki, and N. Assa-Munt. 1999. Mutation analysis of the Pip interaction domain reveals critical residues for protein-protein interactions. *Proc. Natl. Acad. Sci. USA.* 96:2740–2745.
25. Tsujimura, H., T. Tamura, C. Gongora, J. Aliberti, C. Reis e Sousa, A. Sher, and K. Ozato. 2003. ICSBP/IRF-8 retrovirus transduction rescues dendritic cell development in vitro. *Blood.* 101:961–969.
26. Holtschke, T., J. Lohler, Y. Kanno, T. Fehr, N. Giese, F. Rosenbauer, J. Lou, K.P. Knobeloch, L. Gabriele, J.F. Waring, et al. 1996. Immunodeficiency and chronic myelogenous leukemia-like syndrome in mice with a targeted mutation of the ICSBP gene. *Cell.* 87:307–317.
27. Jabado, N., A. Jankowsky, S. Dougaparsad, V. Picard, S. Grinstein, and P. Gros. 2000. Natural resistance to intracellular infections: natural resistance–associated macrophage protein 1 (Nramp1) functions as a pH-dependent manganese transporter at the phagosomal membrane. *J. Exp. Med.* 192:1237–1248.
28. Skamene, E., E. Schurr, and P. Gros. 1998. Infection genomics: *Nramp1* as a major determinant of natural resistance to intracellular infections. *Annu. Rev. Med.* 49:275–287.
29. Malo, D., K. Vogan, S. Vidal, J. Hu, M. Cellier, E. Schurr, A. Fuks, N. Bumstead, K. Morgan, and P. Gros. 1994. Haplotype mapping and sequence analysis of the mouse Nramp gene predict susceptibility to infection with intracellular parasites. *Genomics.* 23:51–61.
30. King, S.R., B.J. Berson, and R. Risser. 1988. Mechanism of interaction between endogenous ecotropic murine leukemia viruses in (BALB/c X C57BL/6) hybrid cells. *Virology.* 162:1–11.
31. Li, M., X. Huang, Z. Zhu, and E. Gorelik. 1999. Sequence and insertion sites of murine melanoma-associated retrovirus. *J. Virol.* 73:9178–9186.
32. Hurt, E.M., A. Wiestner, A. Rosenwald, A.L. Shaffer, E. Campo, T. Grogan, P.L. Bergsagel, W.M. Kuehl, and L.M. Staudt. 2004. Overexpression of c-maf is a frequent oncogenic event in multiple myeloma that promotes proliferation and pathological interactions with bone marrow stroma. *Cancer Cell.* 5:191–199.
33. Scharton-Kersten, T., C. Contursi, A. Masumi, A. Sher, and K. Ozato. 1997. Interferon consensus sequence binding protein–deficient mice display impaired resistance to intracellular infection due to a primary defect in interleukin 12 p40 induction. *J. Exp. Med.* 186:1523–1534.
34. Giese, N.A., L. Gabriele, T.M. Doherty, D.M. Klinman, L. Tadesse-Heath, C. Contursi, S.L. Epstein, and H.C. Morse III. 1997. Interferon (IFN) consensus sequence–binding protein, a transcription factor of the IFN regulatory factor family, regulates immune responses in vivo through control of interleukin 12 expression. *J. Exp. Med.* 186:1535–1546.
35. Schmidt, M., S. Nagel, J. Proba, C. Thiede, M. Ritter, J.F. Waring, F. Rosenbauer, D. Huhn, B. Wittig, I. Horak, and A. Neubauer. 1998. Lack of interferon consensus sequence binding protein (ICSBP) transcripts in human myeloid leukemias. *Blood.* 91:22–29.

36. Deng, M., and G.Q. Daley. 2001. Expression of interferon consensus sequence binding protein induces potent immunity against BCR/ABL-induced leukemia. *Blood*. 97:3491–3497.
37. Hao, S.X., and R. Ren. 2000. Expression of interferon consensus sequence binding protein (ICSBP) is downregulated in Bcr-Abl-induced murine chronic myelogenous leukemia-like disease, and forced coexpression of ICSBP inhibits Bcr-Abl-induced myeloproliferative disorder. *Mol. Cell. Biol.* 20:1149–1161.
38. Schwieger, M., J. Lohler, J. Friel, M. Scheller, I. Horak, and C. Stocking. 2002. AML1-ETO inhibits maturation of multiple lymphohematopoietic lineages and induces myeloblast transformation in synergy with ICSBP deficiency. *J. Exp. Med.* 196:1227–1240.
39. Suzuki, T., H. Shen, K. Akagi, H.C. Morse, J.D. Malley, D.Q. Naiman, N.A. Jenkins, and N.G. Copeland. 2002. New genes involved in cancer identified by retroviral tagging. *Nat. Genet.* 32:166–174.
40. Kanazawa, N., M. Kurosaki, N. Sakamoto, N. Enomoto, Y. Itsui, T. Yamashiro, Y. Tanabe, S. Maekawa, M. Nakagawa, C.H. Chen, et al. 2004. Regulation of hepatitis C virus replication by interferon regulatory factor 1. *J. Virol.* 78:9713–9720.
41. Morse, H.C., III, C.F. Qi, S.K. Chattopadhyay, M. Hori, L. Taddesse-Heath, K. Ozato, J.W. Hartley, B.A. Taylor, J.M. Ward, N.A. Jenkins, et al. 2001. Combined histologic and molecular features reveal previously unappreciated subsets of lymphoma in AKXD recombinant inbred mice. *Leuk. Res.* 25:719–733.
42. Mitsos, L.M., L.R. Cardon, A. Fortin, L. Ryan, R. LaCourse, R.J. North, and P. Gros. 2000. Genetic control of susceptibility to infection with Mycobacterium tuberculosis in mice. *Genes Immun.* 1:467–477.
43. Min-Oo, G., A. Fortin, M.F. Tam, A. Nantel, M.M. Stevenson, and P. Gros. 2003. Pyruvate kinase deficiency in mice protects against malaria. *Nat. Genet.* 35:357–362.
44. Hanna, Z., D.G. Kay, N. Rebai, A. Guimond, S. Jothy, and P. Jolicoeur. 1998. Nef harbors a major determinant of pathogenicity for an AIDS-like disease induced by HIV-1 in transgenic mice. *Cell.* 95:163–175.
45. Epstein, D.J., M. Vekemans, and P. Gros. 1991. Splotch (Sp2H), a mutation affecting development of the mouse neural tube, shows a deletion within the paired homeodomain of Pax-3. *Cell.* 67:767–774.
46. Gros, P., E. Skamene, and A. Forget. 1981. Genetic control of natural resistance to *Mycobacterium bovis* (BCG) in mice. *J. Immunol.* 127:2417–2421.
47. Forget, A., E. Skamene, P. Gros, A.C. Miailhe, and R. Turcotte. 1981. Differences in response among inbred mouse strains to infection with small doses of *Mycobacterium bovis* BCG. *Infect. Immun.* 32:42–47.